Fusion Engineering and Design 8 (1989) 421–427
North-Holland, Amsterdam

EXPERIMENTAL AND ANALYTICAL INVESTIGATIONS OF MASS TRANSPORT PROCESSES OF 12Cr–1 MoVW STEEL IN THERMALLY-CONVECTED LITHIUM SYSTEMS

G.E. BELL, M.A. ABDOU *

University of California, Los Angeles, Department of Mechanical, Aerospace and Nuclear Engineering, Los Angeles, California 90024, USA

P.F. TORTORELLI **

Oak Ridge National Laboratory, Metals and Ceramics Division, PO Box 2008, Oak Ridge, Tennesse 37831-6156, USA

Experimental data on corrosion and mass transport in lithium/12Cr–1 MoVW steel were obtained from two thermal convection loops; one operated from 360 to 505 °C for 3040 h and the other from 525 to 655 °C for 2510 h. The experimental effort was supported by analytical investigations of possible mechanisms of corrosion and mass transport. It was found that mass transfer is not a simple function of temperature and alloy component solubility. Above 580 °C mass transfer appears to be dominated by alloy solubility via the temperature gradient. Between 450 and 580 °C, mass transfer appears to be related to surface reactions involving dissolved carbon and nitrogen in lithium with chromium, and carbides on the steel surface. The corrosion rates, as interperted from weight-change as uniform dissolution, from this work, are significantly lower than those adopted in recent blanket design studies.

1. Introduction

Because of its excellent heat transfer and tritium breeding characteristics, molten lithium has been proposed as both a coolant and breeder material for some blanket designs. However, lithium's compatibility with structure alloys is of concern. Lithium becomes highly corrosive to austenitic alloys such as types 304 and 316 stainless steel above 550 °C, as shown by Hoffman [1]. Ferritic steel alloys have been proposed as a possible solution to the corrosion problem while maintaining the desirable properties of high strength and ease of fabrication. Ferritic steels, such as 12Cr–1MoVW, have been shown by Plekhanov and Fedortsov-Lutikov [2] and Tortorelli and DeVan [3] to be less susceptible to corrosive attack by lithium than the austenitic alloys. However, Tortorelli [4] showed that carburization, decarburization and other mass transfer processes, besides simple solubility-related weight changes, were significant for ferritic alloys such as 12Cr–1MoVW. The purpose of the present study is to investigate corrosion and mass transfer in thermally convected lithium/12Cr–1MoVW systems at temperatures higher than those that have been previously studied and to use the experimental observations to construct a model which explains the observed behavior (see Abdou et al. [5]).

2. Experimental procedure

A schematic of the thermal convection loop (TCL) experimental design is shown in fig. 1. The body of the loop was formed by connecting 3.2 cm ID tubing to a 3500 cm^3 surge tank. The specimens were periodically removed through standpipes on top of the surge tank. The mass transport specimens for the subject investigations were short tubular pieces (1.9 cm OD, 1.8 cm ID × approximately 3.8 cm long). Each loop contained 42 specimens (20 and 22 in the heated and cooled legs, respectively). The specimen surface area to total lithium volume ratio was 34.9 m^{-1} for both loops. The specimens were machined with tongue-and-groove ends and stacked, one on top of the other, to form a continuous

* Research sponsored in part under the U.S. Department of Energy grant number DE-FG03-86ER52123.
** Research sponsored in part by the Office of Fusion Energy, U.S. Department of Energy under contract DE-AC05-84OR21400 with Martin Marietta Energy Systems, Inc.

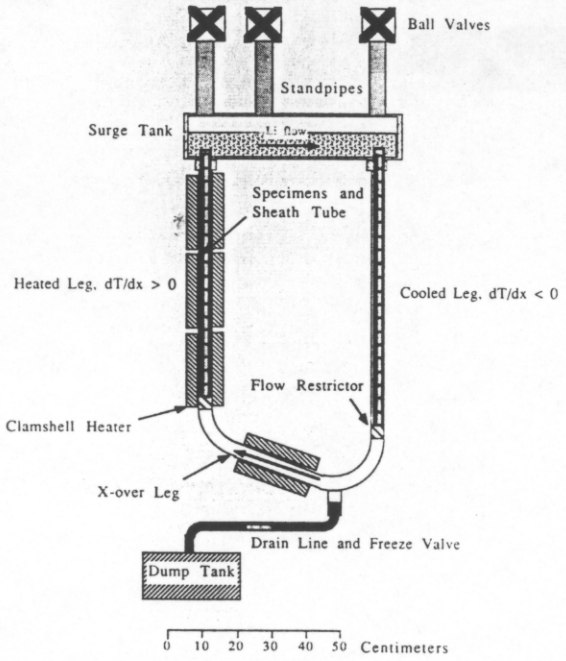

Fig. 1. Schematic of thermal convection loop experiment design.

tube. The stack of specimens is axially supported by a specimen sheath tube which provides a close-fitting annular specimen containment. Prior to insertion in the loops, the specimens were isothermally annealed for 30 min at 1050 °C and 2.5 h at 780 °C in argon and then mechanically polished to 30 and 0.3 μm finishes on the outside and inside surfaces, respectively, to provide the starting microstructure and surface characteristics. Lithium flow was produced in the loops by imposing a temperature gradient between the two vertical legs of the loop. Flow is directed through the inside diameter of the specimens by restricters at the bottom of each leg. All steel in contact with lithium (TCL and specimens) was 12Cr–1MoVW whose composition was determined to be 85Fe–11.9Cr–1.0Mo–0.7Mn–0.4W–0.2V–0.1Si–0.4Ni–0.2C (wt%).

Two TCL experiments were operated simultaneously to cover the desired temperature range. Loops GEB-1 and GEB-2 operated from approximately 360 to 505 °C for 3040 h and 525 to 655 °C for 2510 h, respectively. Lithium velocities were estimated to be (7 ± 2) cm/s, corresponding to average Reynold's number of 1400 for GEB-1 and 1600 for GEB-2.

The lithium used to flush and refill the loops was purified by cold and hot trapping. Typical chemical analyses showed less than 25 and 200 weight parts per million (wppm) for nitrogen and oxygen, respectively.

The specimens were withdrawn at specimen exposure times of 97, 292, 460, 984, 1496, 1996, 2505 and 3040 h for GEB-1 and 95, 292, 459, 1014, 1235, 1497, 1840 and 2510 h for loop GEB-2. Prior to reinsertion, the specimens were cleaned with water and alcohol to remove residual lithium, dried and weighed (± 0.0001 g). Samples of lithium were taken from the experiments several times during the specimen exposure and were analyzed to provide a chemical history of the loops' lithium. A more complete description of the loop fabrication, operation and experimental procedures may be found in Bell [6].

3. Experimental results

Weight change data as a function of specimen position and temperature for selected specimens from the two experiments are shown in figs. 2 and 3. In both figs. 2 and 3, weight change less than zero indicates corrosion (net specimen weight loss) and weight change greater than zero indicates deposition (net specimen weight gain). The open squares depict weight change, the closed squares depict the corresponding specimen temperature, and the arrows point to the appropriate scale. The heading captions refer to the TCL schematic in fig. 1, where $dT/dx < 0$ represents the cooled leg and $dT/dx > 0$ represents the heated leg. Weight changes in GEB-1, $T_{max} = 505$ °C, were more than an order of magnitude smaller than those in GEB-2 with $T_{max} = 655$ °C. Weight-loss occurred for most specimens in the $T_{max} = 505$ °C loop. However, specimens in the heated leg with temperatures greater than approximately 450 °C showed significant weight gains despite being at the highest temperature positions in the loop (fig. 2). Weight loss did not monotonically increase with temperature and mass transfer from the heated leg to the cooled leg was not apparent from the weight change data. In GEB-2 with $T_{max} = 655$ °C, weight losses and gains occurred in both the heated and cooled legs of the loop (fig. 3). Weight losses were recorded for specimens at temperatures above 580 °C and weight gains were measured below 580 °C. The weight loss for temperatures above 580 °C increased rapidly, as compared with the specimens below this temperature (fig. 3).

Fig. 4 shows scanning electron microscope (SEM) micrographs of typical specimen surfaces from the heated and cooled legs of both loops after exposure for 3040 and 2510 h in GEB-1 and GEB-2, respectively. The surfaces of specimens exposed to lithium at temper-

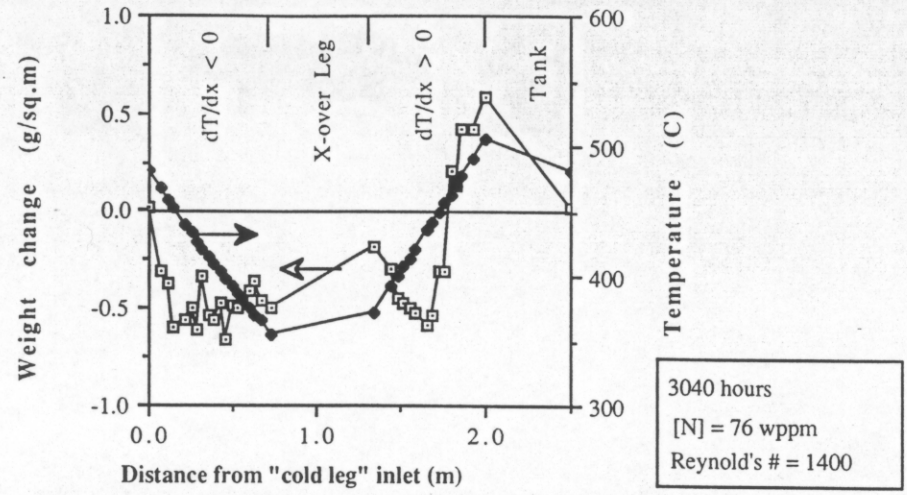

Fig. 2. Weight-change and temperature profile for GEB-1, T_{max} = 505 °C.

atures below 450 °C in GEB-1 were characterized by a "pebbled" or roughened appearance (fig. 4a). Specimens exposed at temperatures between 450 and 505 °C in GEB-1 showed faceted "nodules" which first appeared at the grain boundaries of the pebbled surface (fig. 4b). Semi-quantitative, energy-dispersive X-ray (EDX) analysis of the nodules showed them to be composed of chromium and iron, but chromium-rich in comparison to the base material. The ratio of chromium to iron increased with increasing temperature. X-ray diffraction patterns of specimen surfaces heavily populated with such nodules clearly showed the presence of $M_{23}C_6$ where M may consist of the metallic constituents chromium (Cr) and/or iron (Fe). The presence of these nodules accounted for the net weight gains in the hottest portions of GEB-1. The same type of $M_{23}C_6$ nodules on a pebbled substrate were found on the surfaces of GEB-2 specimens between 530 °C and 570 °C (fig. 4c). Between 570 and 655 °C, and the carbide nodules disappeared and the surface was characterized by larger pebbles (fig. 4d).

EDX analysis of the pebbled specimen surfaces revealed depletion in chromium to between 4 and 10% by weight from the original 11.9%. The amount of chromium depletion from the underlying base material increased with temperature.

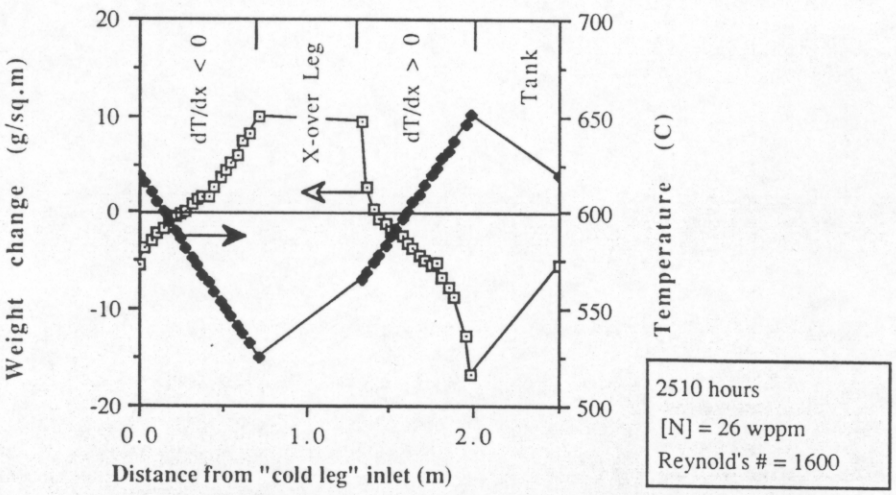

Fig. 3. Weight-change and temperature profile for GEB-2, T_{max} = 655 °C.

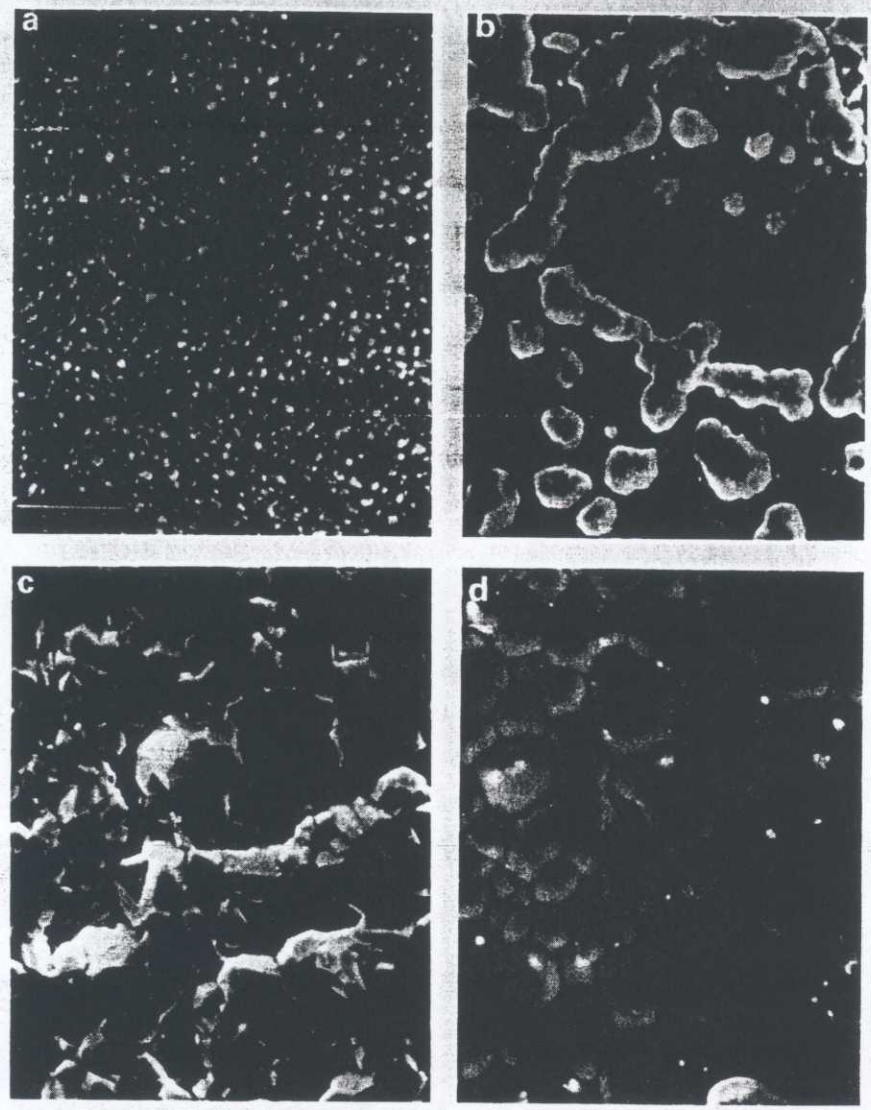

Fig. 4. Scanning electron microscope micrographs of 12Cr–1MoVW steel exposed to lithium. (a) GEB-1, 360 ° C; 3040 h; 2000X. (b) GEB-1, 500 ° C; 3040 h; 2000X (c) GEB-2, 530 ° C; 2510 h; 2000X. (d) GEB-2, 655 ° C; 2510 h; 2000X.

Chemical analyses of the lithium for nitrogen by micro-Kjeldahl showed that the loops reached average steady-state concentrations of 76 and 26 wppm in GEB-1 and GEB-2, respectively. The average oxygen concentrations were determined by fast-neutron activation and increased from approximately 200 to 500 wppm for both GEB-1 and GEB-2, probably due to contamination during sample insertion and removal. However, due to the extreme thermodynamic stability of Li_2O, oxygen does not affect the corrosion of steels in lithium [1].

4. Thermodynamic predictions of corrosion behavior

Increased weight losses in chromium-containing steels with increasing nitrogen in lithium have been determined to be due to the formation of a ternary

lithium–chromium nitride compound on the steel by many investigators. (e.g. Hoffman [1], Barker et al. [7], and Callaway [8]). In particular, Barker et al. [7] has identified the compound to be Li_9CrN_5. We assume the reaction is given in eq. (1).

$$5\ Li_3N + Cr \rightarrow Li_9CrN_5 + 6\ Li. \quad (1)$$

The free energy of formation for eq. (1) can be obtained by subtracting the free energy of the products from the reactants. Based on free energy data of Pulham and Watson [9] and Natesan [10], activity data for chromium in steels, and assuming lithium nitride obeys Henry's Law, it is possible to predict the theoretical equilibrium nitrogen concentration in lithium at which Li_9CrN_5 forms on a chromium containing steel. The resulting curve is plotted in fig. 5 along with the average surgetank nitrogen levels for both GEB-1 and GEB-2 as determined by the micro-Kjeldahl method. The curve is consistent with the surgetank nitrogen level measured in loop GEB-1. Such agreement strongly indicates that the corrosion reaction shown in eq. (1) determined the nitrogen concentration of the GEB-1 experiment and thus plays an important role in the overall corrosion and mass transfer processes for this system. This curve indicates that at temperatures below 450 °C if samples of a chromium-bearing alloy are brought into contact with lithium containing more than 80 wppm nitrogen, then a weight loss will occur due to the formation and subsequent removal during cleaning of the insoluble ternary compound, Li_9CrN_5, and not simply because of the dissolution of the alloy components in the lithium. On the other hand, if a chromium alloy forms, the ternary compound surface layer at some temperature where the equilibrium nitrogen concentration is [N*] and then is contacted with lithium containing nitrogen [N], such that [N*] > [N], then the ternary compound will decompose into Li_3N in Li and chromium on the surface of the steel in order to try and regain equilibrium, or if the ternary compound is not present then it cannot form because the nitrogen activity is too low. Such a process can occur in loop systems with large temperature differentials ($\Delta T > 100$ °C), where there is a flow of lithium from regions with different equilibrium nitrogen contents. Further investigation of the roles of the ternary corrosion product and dissolved carbon on the formation of the $M_{23}C_6$ nodules is warranted by these results (see [6]).

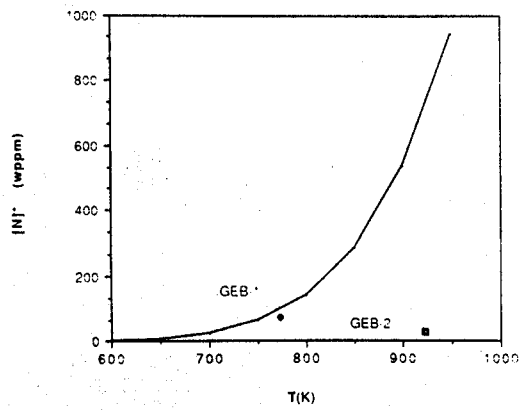

Fig. 5. Equilibrium nitrogen concentration in lithium for reaction $5\ Li_3N + Cr \rightarrow Li_9CrN_5 + 6\ Li$ with chromium on steel.

5. Discussion

Solubility-driven thermal gradient mass transfer (i.e. mass removal in the heated leg and deposition in the cooled leg by differences in solubility) did not appear to be significant in GEB-1 with $T_{max} = 505$ °C. The weight change data in fig. 3 for GEB-2 with $T_{max} = 655$ °C showed both mass removal and deposition occurring throughout the loop. Thermal gradient mass transfer did appear significant at the higher temperatures of GEB-2. Similar changes in behavior as a function of T_{max} had been earlier observed in TCL experiments with 12Cr–1MoVW characterized by lower lithium temperature, mass flow rate and Reynold's number by Tortorelli [3,4]. The magnitude of the weight changes in this investigation was consistent with previous investigations at lower temperatures (Chopra and Smith [11,12], Tortorelli and DeVan [3] and Tortorelli [4]). However, mass transfer rates and weight changes were between a factor of 4 or 5 lower than were estimated in design studies (e.g. Smith et al. [13]).

As discussed in Section 4, equilibrium between the steel and lithium determines the nitrogen content of the loops in the low temperature experiment. Small weight losses below 450 °C were probably due to formation of an adherent, protective film of Li_9CrN_5 (Barker et al. [7]) during loop operation and the subsequent removal of the film during specimen cleaning. This would account for the near uniform weight losses between 360 and 450 °C. At higher temperatures, above 570 °C, the behavior is more indicative of solubility-driven dissolution transport. This behavior would indicate that the Li_9CrN_5 is less adherent at the higher temperatures or, alternatively, that nitrogen at the levels found here no longer control the corrosion (i.e. Li_9CrN_5 can no longer form as indicated by the point for GEB-2 in fig. 5).

The appearance of the exposed specimens is also similar to that which was previously investigated. The "pebbled" base material surface beneath the faceted nodules persists on all the specimens exposed to lithium in this and other studies by Tortorelli [4] with ferritic alloys. The size of the surface pebbles was seen to increase with increasing temperature (figs. 4a–4d). Surface chromium contents were highest at intermediate temperatures where the $M_{23}C_6$ nodules are found. It is not clear whether the observations of chromium depletion, surface "pebbling" and $M_{23}C_6$ nodule formation were related. However, surface chromium content decreased with increasing pebble size and temperature.

As noted above, the $M_{23}C_6$ nodules were only present at temperatures between 450 and 570 °C, and growth of these carbide nodules accounts for the net weight gains in hottest portion of GEB-1. The nodules appeared first and disappeared last at the grain boundaries of the specimens where carbides on the steel surface served as nucleation sites for subsequent growth. Qualitatively, more nodules were present on the GEB-2 than the GEB-1 specimens. The fact that more nodules appear in the higher T_{max} system was probably due to more chromium and carbon available from dissolution and decarburization processes which readily occurred at the higher temperatures. The chromium to iron ratios of the surface $M_{23}C_6$ nodules were consistent with those found in 12Cr–1MoVW by Vitek and Klueh [14]. The similarity of such features to those observed in independent loop experiments of Tortorelli and DeVan [3], Tortorelli [4] and Chopra and Smith [11,12] emphasizes the importance of chromium and carbon reactions and subsequent transport (possibly via ternary nitride corrosion product and $M_{23}C_6$ nodule formation) in the temperature range of interest for ferrous alloy–lithium systems, as has been suggested previously by Barker et al. [7] and Tortorelli [4].

As discussed by Bell [6] and Bell et al. [15], the formation of $M_{23}C_6$ deposits may be related to surface products from reactions with nitrogen and pre-existing carbides, particularly at the grain boundaries, on the steel surface. The temperatures (450 to 570 °C) at which the nodules occur are near the 520 °C (sigma-phase) solidus [16] phase boundary and the theoretical maximum of the equilibrium nitrogen in lithium (eq. (1)) as indicated by fig. 5. The presence of lithium and/or a lithium/nitrogen/chromium corrosion product may affect the kinetics of the carbide phase formation and growth. In particular, a change in chromium solubility at the 520 °C solidus may decrease chromium activity on the steel surface. However, regardless of the mechanism by which such nodules form, it is apparent that the formation of the surface nodules and other surface reactions must be considered in any mass transfer model of lithium–Fe–Cr(–Ni, Mn) systems and, specifically, in the design of heat transport systems utilizing Fe–Cr alloys with lithium.

6. Conclusions

(1) Mass transfer in lithium/12Cr–1MoVW systems is not simply a function of temperature nor is it simply solubility driven. Absolute temperature as well as temperature differential are both important.

(2) Mass transfer in systems operating above ~ 580 °C appears to be controlled by temperature gradient mass transfer from higher to lower temperature regions. Between 450 and 580 °C, mass transfer appears to be related to surface reactions involving carbon and nitrogen in the lithium and chromium, and carbides, on the steel. Below 450 °C, weight loss may be due to formation and removal of the Li_9CrN_5 corrosion product on the steel surface.

(3) Corrosion rates, as interpreted as a uniform dissolution rate, were not as severe as estimated in recent design studies.

(4) Exposure of 12Cr–1MoVW to lithium produced a "pebbled" base material surface for all specimens. The size of the pebbles increased with temperature and ranged in size from 0.10 to 10 s of μm Resulting surface chromium contents were between 4 and 10 wt%. Formation of $M_{23}C_6$ nodules occurs over a very specific temperature range of 450 to 570 °C. This range is close to the theoretical maximum of the nitrogen concentration in lithium in equilibrium with Li_9CrN_5 and includes the sigma-phase solidus phase boundary on the Fe–Cr phase diagram.

(5) The formation of surface $M_{23}C_6$ nodules as well as the role of the chromium reaction products must be considered in any mass transfer model of Li/Fe–Cr(–Ni, Mn) systems and, specifically, in the design of heat transport systems utilizing Fe–Cr alloys with lithium.

References

[1] E.E. Hoffman, Corrosion of materials by lithium at elevated temperatures, Oak Ridge National Laboratory Report, ORNL-2924 (1960).

[2] G.A. Plekhanov and G.P. Fedortsov-Lutikov, Corrosion of 12% chromium steel in a nonisothermal lithium flow, At. Energiya 45 (1978) 140–144.

[3] P.F. Tortorelli and J.H. DeVan, Corrosion of an Fe–12Cr–1MoVW steel in thermally convective lithium, in: Proc. Topical Conf. on Ferritic Alloys for Use in Nuclear Energy Applications, eds. J.W. Davis and D.J. Michel (AIME, 1984) pp. 215–221.

[4] P.F. Tortorelli, Corrosion of ferritic steels by molten lithium: influence of competing thermal gradient mass transfer and surface product reactions, in: Proc. Third Internat. Conf. on Fusion Reactor Materials, Karlsruhe, Federal Republic of Germany, October 4–8, 1987, to be published in J. Nucl. Mater. (1988).

[5] M.A. Abdou et al., Modeling, analysis and experiments for fusion nuclear technology, FNT Progress Report: Modeling & FINESSE, PPG-1021, UCLA-ENG-86-44, FNT-17 (January 1987).

[6] G.E.C. Bell, Thermal convection loop experiments and analysis of mass transport processes in lithium/Fe–12 Cr–1 MoVW systems, PhD dissertation, University of California, Los Angeles (1988).

[7] M.G. Barker et al., The interaction of chromium with nitrogen dissolved in liquid lithium, J. Nucl. Mater. 114 (1983) 143.

[8] W.F. Callaway, The reaction of chromium with lithium nitride in liquid lithium, in: Proc. 2nd Internat. Conf. on Liquid Metal Technology in Energy Production, ed. J. M. Dahlke (U. S. DOE, CONF-800401-P2, 1980) pp. 18-18–18-26.

[9] R.J. Pulham and W.R. Watson, Corrosion of 316 steel by lithium–lead alloys under nitrogen, in: 14th Symp. on Fusion Nuclear Technology Abstract, Avignon, France, September 8–12, 1986 (1987).

[10] K. Natesan, Influence of nonmetallic elements on the compatibility of structural materials with liquid alkali metals, J. Nucl. Mater. 115 (1983) 251–262.

[11] O.K. Chopra and D.L. Smith, Influence of temperature and lithium purity on corrosion of ferrous alloys in a flowing lithium environment, J. Nucl. Mater. 141–143 (1986) 584–591.

[12] O.K. Chopra and D.L. Smith, Compatibility of ferritic steels in forced circulation lithium and Pb–17Li Systems, in: Proc. Third Internat. Conf. on Fusion Reactor Materials, Karlsruhe, Federal Republic of Germany, October 4–8, 1987, to be published in J. Nucl. Mater. (1988).

[13] D.L. Smith et al., Blanket comparison and selection study-final report, Argonne National Laboratory Report, ANL/FPP-84-1 (September 1984).

[14] J.M. Vitek and R.L. Klueh, Precipitation reactions during the heat treatment of ferritic steels, Metall. Trans. 14A (June 1983) 1047–1055.

[15] G.E. Bell, P.F. Tortorelli and M.A. Abdou, Corrosion and mass transfer in lithium-12Cr-1MoVW steel systems, in: Fusion Reactor Material Semiannual Progress Report for the period ending September 30, 1987, DOE/ER-0313/3 (1987).

[16] R.P. Elliot, Constitution of Binary Alloys, First Supplement (McGraw-Hill, New York, 1965).